

Perfect quantum state transfer on diamond fractal graphs

Maxim Derevyagin¹, Gerald V. Dunne^{1,2}, Gamal Mograby¹
 Alexander Teplyaev^{1,2}

December 21, 2024

Affiliation:

¹Mathematics Department, University of Connecticut, Storrs CT 06269

²Physics Department, University of Connecticut, Storrs CT 06269.

Email: maksym.derevyagin@uconn.edu gerald.dunne@uconn.edu
 gamal.mograby@uconn.edu alexander.teplyaev@uconn.edu

Abstract

We extend the analysis of perfect quantum state transfer beyond one dimensional spin chains to show that it can be achieved and designed on a large class of fractal structures, known as diamond fractals, which have a wide range of Hausdorff and spectral dimensions. The resulting systems are spin networks combining Dyson hierarchical model structure with transverse permutation symmetries of varying order.

1 Introduction

The study of state transfer was initiated by S. Bose [1, 2], who considered a $1D$ chain of N qubits coupled by the time-independent Hamiltonian. The main idea is to transport a quantum state from one end of the chain to the other. The transport of the quantum state from one location to another is called perfect if it is realized with probability 1, that is, without dissipation. In addition to its fundamental interest, this means that perfect quantum state transfer also has potential applications to the design of sub-protocols for quantum information and quantum computation [3–5]. A number of one dimensional cases, when perfect transmission can be achieved, have been found in some XX chains with inhomogeneous couplings, see [2, 3, 6–15, and references therein]. These models have the advantage that the perfect transfer can be done without the need for active control. Recently there has been active interest to generalize these results to graphs with potentials and to graphs that are not one dimensional [5, 16–18]. These works illustrate the fact that perfect state transfer is a rare phenomenon, for which the construction of explicit examples remains rather non-trivial.

The main result of our paper is to show that perfect quantum state transfer is possible on the large and diverse class of fractal-type diamond graphs, which have different geometrical

properties including a wide range of dimensions. These graphs have provided an important collection of structures with interesting physical and mathematical properties and a broad variety of geometries, see [19–27] and Figures 1, 2, 4. The structure of these graphs is such that they combine spectral properties of Dyson hierarchical models and transport properties of one dimensional chains. The methods that we use are discretized versions of the methods recently developed in [23, 24] (see also [29, 30]), which provides a construction of Green’s functions for diamond fractals. Our work is part of a long term study of mathematical physics on fractals and self-similar graphs [20, 31–39], in which novel features of quantum processes on fractals can be associated with the unusual spectral and geometric properties of fractals compared to regular graphs and smooth manifolds.

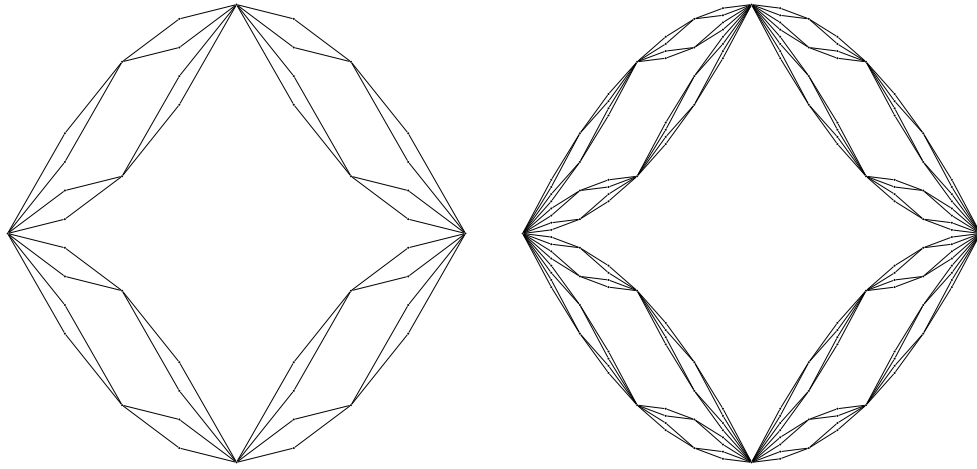


Figure 1: The most standard diamond hierarchical fractal graphs with the similarity dimension $\dim = 2$, [31, Section 7] and [19–23, 25]. (Left: graph level 3, right: graph level 4)

2 1-D Chains

We begin with a brief summary of perfect quantum state transfer on 1 D chains [3]. Consider one dimensional Hamiltonians \mathbf{H} of the XX type with nearest-neighbor interactions

$$\mathbf{H} = \frac{1}{2} \sum_{n=0}^{N-1} J_{n+1} (\sigma_n^x \sigma_{n+1}^x + \sigma_n^y \sigma_{n+1}^y) + \frac{1}{2} \sum_{n=0}^N B_n (\sigma_n^z + 1),$$

where J_n are the constants coupling the sites $(n-1)$ and n , and B_n are the strengths of the magnetic field at the sites n ($n = 0, 1, \dots, N$). The symbols σ_n^x , σ_n^y , σ_n^z denote the standard Pauli matrices which act as follows on the single qubit states $|\downarrow\rangle$ and $|\uparrow\rangle$:

$$\begin{aligned} \sigma^x |\downarrow\rangle &= |\uparrow\rangle, & \sigma^y |\downarrow\rangle &= -i |\uparrow\rangle, & \sigma^z |\downarrow\rangle &= -|\downarrow\rangle \\ \sigma^x |\uparrow\rangle &= |\downarrow\rangle, & \sigma^y |\uparrow\rangle &= i |\downarrow\rangle, & \sigma^z |\uparrow\rangle &= |\uparrow\rangle. \end{aligned}$$

It is straightforward to see that $[\mathbf{H}, \sum_{n=0}^N (\sigma_n^z + 1)] = 0$ and so the eigenstates of \mathbf{H} split in subspaces labeled by the number of spins over the chain that are in state $|\uparrow\rangle$. It suffices to restrict \mathbf{H} to the subspace spanned by the states that contain only one excitation. A natural basis for that subspace is given by the vectors $|n\rangle = (0, 0, \dots, 1, \dots, 0)$, $n = 0, 1, 2, \dots, N$, where the only " \uparrow " occupies the n -th position. In this basis, the restriction \mathbf{J} of \mathbf{H} to the one-excitation subspace is given by the following $(N+1) \times (N+1)$ symmetric tridiagonal matrix

$$\mathbf{J} = \begin{pmatrix} B_0 & J_1 & & & \mathbf{0} \\ J_1 & B_1 & J_2 & & \\ & J_2 & B_2 & \ddots & \\ & & \ddots & \ddots & J_N \\ \mathbf{0} & & & J_N & B_N \end{pmatrix}. \quad (1)$$

Such matrices are called Jacobi matrices and, as usual for the theory of Jacobi matrices, we assume that $J_n > 0$ for $n = 1, 2, \dots, N$. Clearly, the action of the operator \mathbf{J} on the basis vectors $|n\rangle$ gives

$$\mathbf{J}|n\rangle = J_{n+1}|n+1\rangle + B_n|n\rangle + J_n|n-1\rangle,$$

for $n = 0, 1, \dots, N$, where we set $J_0 = J_{N+1} = 0$. Now we can see that after some time t the initial state will evolve into the state $e^{it\mathbf{J}}|0\rangle$. So, in order to transfer an excitation from the site $|0\rangle$ to the site $|N\rangle$ there should exist $T > 0$ and $\phi \in \mathbb{R}$ such that

$$e^{iT\mathbf{J}}|0\rangle = e^{i\phi}|N\rangle. \quad (2)$$

As was noted in [3] the latter condition immediately implies that the entries of the Jacobi matrix J satisfy the following relations

$$B_n = B_{N-n}, \quad J_n = J_{N+1-n}, \quad n = 1, 2, \dots, N,$$

which is the mirror symmetry of the matrix \mathbf{J} . This property can also be expressed in the following way

$$\mathbf{J} = \mathbf{R}\mathbf{J}\mathbf{R},$$

where the matrix \mathbf{R} , the mirror reflection matrix, is

$$\mathbf{R} = \begin{pmatrix} 0 & 0 & \dots & 0 & 1 \\ 0 & 0 & \dots & 1 & 0 \\ \vdots & \vdots & \ddots & \vdots & \vdots \\ 0 & 1 & \dots & 0 & 0 \\ 1 & 0 & \dots & 0 & 0 \end{pmatrix}.$$

Furthermore, in [3] the following necessary and sufficient conditions for state transfer in the chain corresponding to the mirror symmetric Jacobi matrix \mathbf{J} was proved: the ordered set of the eigenvalues λ_k of \mathbf{J} ($\lambda_{k-1} < \lambda_k$) must satisfy

$$\lambda_k - \lambda_{k-1} = (2m_k + 1)\pi/T, \quad k = 1, 2, \dots, N, \quad (3)$$

where T is the state transfer time, and m_k is a nonnegative integer, which can vary with k .

As an example we can consider one of the simplest cases of spin chains with perfect state transfer discussed in [6]. To this end, let us set

$$J_n = \frac{\sqrt{n(N+1-n)}}{2}, \quad B_n = 0 \quad (4)$$

and so the underlying Jacobi matrix is mirror symmetric and it corresponds to the symmetric Krawtchouk polynomials [40]. Also, it is known that in this case we have that

$$\lambda_k = k - N/2, \quad k = 0, 1, \dots, N, \quad (5)$$

and, thus, $\lambda_k - \lambda_{k-1} = 1$, which means that the condition (3) is satisfied with $T = \pi$. As a result, the corresponding 1D spin system can realize perfect state transfer with the transfer time $T = \pi$. For more examples of spin chains with perfect transfer, see [3, 18] and references therein.

3 Hamiltonians on Graphs

We extend the results mentioned above to a collection of fractal-type diamond graphs. These graphs are no longer one dimensional, so they can be used to study more complex quantum systems as an extension to the 1D spin chain models. Indeed, the diamond fractals can have a wide variety of dimensions for different choices of their self-similar structure. We equip these graphs with a general Hamiltonian that encodes their geometric information and takes the fractal-type diamond graph symmetries into account. Our main result in this paper is to show that perfect state transfer on this collection of fractal-type diamond graphs can be reduced to an appropriately constructed 1D chain. We effectively separate variables into a longitudinal direction and transverse directions related to a hierarchy of permutation symmetries. This separation leads to conditions that are sufficient to both *construct* and *design* these general Hamiltonians in such a way that guarantees perfect state transfer.

The class of fractal-type diamond graphs studied in [23] is a family of graphs $\{G_l\}_{l \geq 0}$ which is characterized by two sequences of numbers: a sequence of *branching parameters* $\{\mathcal{N}_l\}_{l \geq 0}$, and a sequence of *segmenting numbers* $\{\mathcal{J}_l\}_{l \geq 0}$. Each link on the graph branches into a given number of links, and is also segmented into a given number of links. See Figures 1, 2 for some examples that illustrate this structure. These sequences generate inductively $\{G_l\}_{l \geq 0}$ in the following sense. At level l we construct G_l by replacing each edge from the previous level G_{l-1} by \mathcal{N}_l new branches, whereas each new branch is then segmented into \mathcal{J}_l edges that are arranged in series. For our purposes in this paper, we will initialize G_0 as the one edge graph connecting two nodes. For example let $\mathcal{N}_l = \mathcal{J}_l = 2$ for all levels $l \in \mathbb{N}$ and G_0 be the one edge graph connecting a node x_L with another node x_R . A construction of the first three levels is schematized in Fig 2. These graphs are fractal-type in the sense that the sequence $\{G_l\}_{l \geq 0}$ approximates a limit graph which is a special diamond fractal, see Figure 1 for higher levels [20].

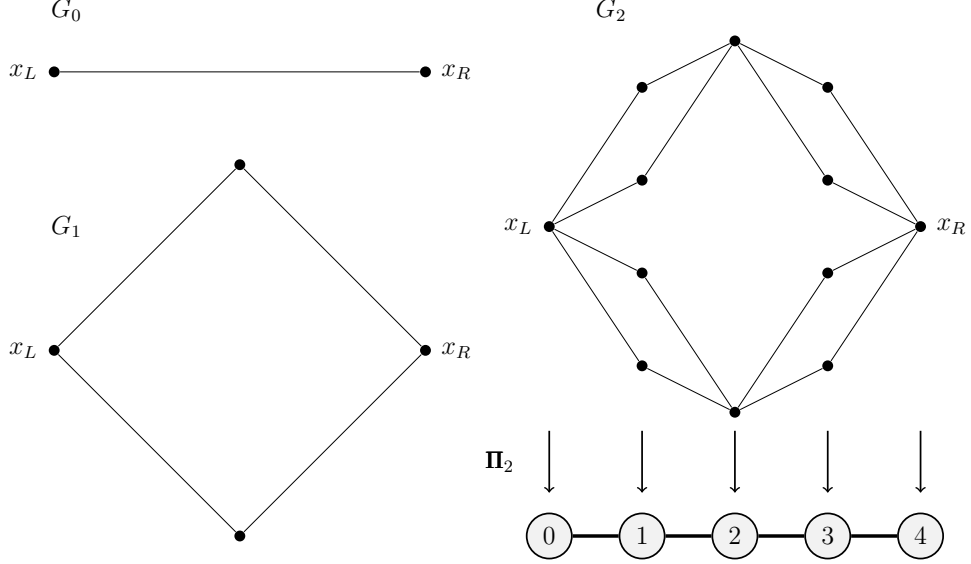


Figure 2: A construction of the first three levels G_0 , G_1 , G_2 and the mapping Π_2

Let V_l denote the set of nodes of the diamond graph G_l . We define the mapping $\Pi_l : V_l \rightarrow \{0, \dots, N\}$ which assigns each node $x \in V_l$ the number of edges of the shortest path from x to the node x_L . For the most standard fractal-type diamond graphs in Figure 1 we have $N = 2^l$. This is not true in general; e.g., for the fractal-type graph in Figure 4 we have $N = 4^l$. For level two the mapping Π_2 is demonstrated in Figure 2. The set of nodes V_l is decomposed into a disjoint union of $N + 1$ intrinsically transversal layers induced by the preimages of Π_l , i.e. $V_l = \{\Pi_l^{-1}(0) \cup \Pi_l^{-1}(1) \dots \cup \Pi_l^{-1}(N)\}$. In particular, when a node is in the transversal layer $\Pi_l^{-1}(n)$, then it has an intrinsic distance of n edges to the node x_L .

A quantum state on G_l is represented by a complex-valued wave function on the nodes V_l . The space of quantum states is defined by

$$L^2(G_l) = \{\psi \mid \psi : V_l \rightarrow \mathbb{C}\}$$

which is a Hilbert space equipped with the inner product

$$\langle \psi | \varphi \rangle_{G_l} = \sum_{x \in V_l} \psi(x) \overline{\varphi(x)} \mu_l(x) \quad (6)$$

where the weights are given by $\mu_l(x) = \frac{1}{|\Pi_l^{-1}(n)|}$ for $n = \Pi_l(x)$ and $|\Pi_l^{-1}(n)|$ denotes the number of nodes in the transversal layer $\Pi_l^{-1}(n)$ that contains x . This factor accounts for the transverse degeneracies due to the permutation symmetries at a given level l . We denote by $|x\rangle$ the wave function that assigns one to the node $x \in V_l$ and zeros elsewhere (one-excitation state on G_l). The set of all one-excitation states $\{|x_L\rangle, \dots, |x_R\rangle\}$ form a natural basis for $L^2(G_l)$.

An l -level Hamiltonian on G_l is a Hermitian operator \mathbf{H}_l acting on $L^2(G_l)$. To encode the geometric information of the fractal-type diamond graph G_l in the Hamiltonian, we impose the following assumptions on \mathbf{H}_l :

- *Nearest-neighbor coupling*: for $x, y \in V_l$, let $\langle x | \mathbf{H}_l | y \rangle_{G_l} = 0$ if x and y are not connected by an edge, i.e. the transition matrix element from quantum state $|y\rangle$ to $|x\rangle$ is zero if the nodes y and x are not adjacent in G_l .
- *Symmetric coupling*: for $x_1, y_1, x_2, y_2 \in V_l$ such that both x_1, y_1 and x_2, y_2 are adjacent, let

$$\langle x_1 | \mathbf{H}_l | y_1 \rangle_{G_l} = \langle x_2 | \mathbf{H}_l | y_2 \rangle_{G_l}$$

if $\mathbf{\Pi}_l(x_1) = \mathbf{\Pi}_l(x_2)$ and $\mathbf{\Pi}_l(y_1) = \mathbf{\Pi}_l(y_2)$,

i.e. the transition matrix element are compatible with the intrinsically transversal layers of G_l .

This means that we can regard $\{0, \dots, N\}$ as the set of nodes of a 1D chain. To reduce the perfect state transfer problem from the graph G_l to this 1D chain, we introduce the following Hilbert space $L^2(\{0, \dots, N\}) = \{\psi \mid \psi : \{0, \dots, N\} \rightarrow \mathbb{C}\}$ equipped with the inner product

$$\langle \psi | \varphi \rangle_l = \sum_{n=0}^N \psi(n) \overline{\varphi(n)}. \quad (7)$$

Moreover we project a wave function in $L^2(G_l)$ to a wave function in $L^2(\{0, \dots, N\})$ through averaging its values on the transversal layers,

$$\begin{aligned} P_l : L^2(G_l) &\rightarrow L^2(\{0, \dots, N\}) \\ \psi &\mapsto P_l \psi(n) = \frac{1}{|\mathbf{\Pi}_l^{-1}(n)|} \sum_{x \in \mathbf{\Pi}_l^{-1}(n)} \psi(x). \end{aligned}$$

A simple calculation using the definition of the inner products gives $\langle P_l \psi | \varphi \rangle_l = \langle \psi | P_l^* \varphi \rangle_{G_l}$, where the adjoint operator P_l^* of P_l is defined by

$$\begin{aligned} P_l^* : L^2(\{0, \dots, N\}) &\rightarrow L^2(G_l) \\ \varphi &\mapsto P_l^* \varphi(x) = \varphi(\mathbf{\Pi}_l(x)). \end{aligned}$$

4 Main results

The Hamiltonian \mathbf{H}_l on G_l induces an operator on the 1D chain $\{0, \dots, N\}$ by

$$\mathbf{J}_l = P_l \mathbf{H}_l P_l^*$$

which acts on $L^2(\{0, \dots, N\})$, see Figure 3. We denote the one-excitation states in $L^2(\{0, \dots, N\})$ by $|n\rangle$ for a node $n \in \{0, \dots, N\}$. Let $\mathbf{H}_l = (H_l(x, y))_{x, y \in V_l}$ be the matrix representation of \mathbf{H}_l with respect to $\{|x_L\rangle, \dots, |x_R\rangle\}$. The following result relates the matrix elements of \mathbf{H}_l to \mathbf{J}_l .

$$\begin{array}{ccc}
L^2(\{0, \dots, N\}) & \xrightarrow{\mathbf{J}_l} & L^2(\{0, \dots, N\}) \\
P_l^* \downarrow & & \uparrow P_l \\
L^2(G_l) & \xrightarrow{\mathbf{H}_l} & L^2(G_l)
\end{array}$$

Figure 3: A diagram to explain the mapping between the Hamiltonian \mathbf{H}_l on the diamond fractal graph G_l and the effective Hamiltonian \mathbf{J}_l on the associated one-dimensional spin chain. The definition of $\mathbf{J}_l = P_l \mathbf{H}_l P_l^*$: we apply first P_l^* , then \mathbf{H}_l , and finally P_l .

Proposition 1. *Let $x \in V_l$,*

1. $H_l(x, x) = \langle \mathbf{H}_l(x) | \mathbf{J}_l | \mathbf{H}_l(x) \rangle_l$.
2. *Let $y \in V_l$ be adjacent to x and $\mathbf{H}_l(y) = \mathbf{H}_l(x) \pm 1$, then*

$$H_l(x, y) = \frac{1}{\deg_{\pm}(x)} \langle \mathbf{H}_l(x) | \mathbf{J}_l | \mathbf{H}_l(x) \pm 1 \rangle_l,$$

where $\deg_{\pm}(x)$ is defined as follows: let $x \in \mathbf{H}_l^{-1}(n)$ for some $n \in \{0, \dots, N-1\}$ the mapping $\deg_+(x)$ assigns the node x the number of edges that connect x to nodes in $\mathbf{H}_l^{-1}(n+1)$. Similarly $\deg_-(x)$ assigns the node x the number of edges that connect x to nodes in $\mathbf{H}_l^{-1}(n-1)$.

3. *The Hamiltonian \mathbf{H}_l is self-adjoint with respect to the inner product 6 if and only if \mathbf{J}_l is self-adjoint with respect to the inner product 7.*

The following result justifies the reduction of the perfect transfer problem from G_l to a 1D chain.

Theorem 1. *If the perfect state transfer on the 1D chain $\{0, \dots, N\}$ is achieved, i.e. there exists $T_l > 0$ such that*

$$e^{iT_l \mathbf{J}_l} |0\rangle = e^{i\phi} |N\rangle$$

for some phase ϕ , then the perfect state transfer on G_l is also achieved with the same time T_l and phase ϕ , i.e.

$$e^{iT_l \mathbf{H}_l} |x_L\rangle = e^{i\phi} |x_R\rangle \quad \text{and} \quad e^{iT_l \mathbf{H}_l} |x_R\rangle = e^{i\phi} |x_L\rangle.$$

5 Proofs

For the purpose of proving the main results, we introduce first the following auxiliary definitions and lemmas. We define the space of functions $\psi \in L^2(G_l)$ that are constant on each transversal layer $\mathbf{H}_l^{-1}(n)$ for $n \in \{0, \dots, N\}$ and denote it by

$$L^2_{\text{sym}}(G_l) = \{\psi \mid \psi(x) = \psi(y) \text{ if } \mathbf{H}_l(x) = \mathbf{H}_l(y)\}.$$

$L^2_{sym}(G_l)$ is a subspace of $L^2(G_l)$ and let $\mathbf{Proj}_l : L^2(G_l) \rightarrow L^2_{sym}(G_l)$ be the projection of $L^2(G_l)$ onto $L^2_{sym}(G_l)$.

Lemma 2. $L^2_{sym}(G_l)$ is an invariant subspace of $L^2(G_l)$ under \mathbf{H}_l .

Proof. Let $\Pi_l^{-1}(n) = \{x_{n_1}, \dots, x_{n_m}\}$ for some $n \in \{0, \dots, N-1\}$ and $|\psi\rangle = |x_{n_1}\rangle + \dots + |x_{n_m}\rangle$, i.e., for $x \in V_l$

$$\langle x|\psi\rangle_{G_l} = \begin{cases} \frac{1}{|\Pi_l^{-1}(n)|} & \text{if } x \in \Pi_l^{-1}(n) \\ 0 & \text{otherwise} \end{cases}$$

It suffices to show that $\mathbf{H}_l|\psi\rangle \in L^2_{sym}(G_l)$. By the symmetric coupling assumption on \mathbf{H}_l we set $c_n = \langle x_{n_1}|\mathbf{H}_l|x_{n_1}\rangle_{G_l} = \dots = \langle x_{n_m}|\mathbf{H}_l|x_{n_m}\rangle_{G_l}$. Note that any two nodes in the same transversal layer are not adjacent. Similarly, for the neighboring transversal layers, we set $c_{n-1} = \langle x|\mathbf{H}_l|y\rangle_{G_l}$ for any adjacent nodes $x \in \Pi_l^{-1}(n-1), y \in \Pi_l^{-1}(n)$ for $n > 0$ and $c_{n+1} = \langle x|\mathbf{H}_l|y\rangle_{G_l}$ for any adjacent nodes $x \in \Pi_l^{-1}(n+1), y \in \Pi_l^{-1}(n)$ for $n < N$. One can easily verify the following formula,

$$\langle x|\mathbf{H}_l|\psi\rangle = \begin{cases} \deg_{+,n-1}c_{n-1} & \text{if } x \in \Pi_l^{-1}(n-1) \\ c_n & \text{if } x \in \Pi_l^{-1}(n) \\ \deg_{-,n+1}c_{n+1} & \text{if } x \in \Pi_l^{-1}(n+1) \\ 0 & \text{otherwise} \end{cases}$$

where the last case is implied by the nearest-neighbor coupling assumption on \mathbf{H}_l and $\deg_{+,n-1}$ (or $\deg_{-,n+1}$) is the number of edges that connect a node in $\Pi_l^{-1}(n-1)$ (or $\Pi_l^{-1}(n+1)$) to nodes in $\Pi_l^{-1}(n)$. \square

Lemma 3. The range of P_l^* is $L^2_{sym}(G_l)$.

Proof. It follows by the definition of P_l^* and $L^2_{sym}(G_l)$. \square

Corollary 4. $\text{Ker } P_l = (L^2_{sym}(G_l))^\perp$. In particular, if $\psi \in (L^2_{sym}(G_l))^\perp$, then the sum over a transversal layer gives $\sum_{x \in \Pi_l^{-1}(n)} \psi(x) = 0$ for $n \in \{0, \dots, N\}$.

Proof. It follows with $\text{Ker } P_l = (\text{Range } P_l^*)^\perp$ and Lemma 3. \square

Lemma 5. Let $\psi \in L^2(G_l)$ and $x \in V_l$, then $P_l^* P_l \psi(x) = \mathbf{Proj}_l \psi(x)$.

Proof. We decompose $\psi = \psi_{sym} + \psi_{sym}^\perp$ such that $\psi_{sym} \in L^2_{sym}(G_l)$ and $\psi_{sym}^\perp \in (L^2_{sym}(G_l))^\perp$. Corollary 4 implies $P_l^* P_l \psi = P_l^* P_l \psi_{sym}$. Let $n \in \{0, \dots, N\}$ and $x \in \Pi_l^{-1}(n)$. Then ψ_{sym} is constant on the transversal layer $\Pi_l^{-1}(n)$ and it's averaging gives $P_l \psi_{sym}(n) = \psi_{sym}(x)$. Hence, by the definition of P_l^* , it follows $P_l^* P_l \psi_{sym}(x) = \psi_{sym}(x) = \mathbf{Proj}_l \psi(x)$. \square

Proof of Proposition 1. Let $x \in \Pi_l^{-1}(n) = \{x_{n_1}, \dots, x_{n_m}\}$ for some $n \in \{0, \dots, N-1\}$. We evaluate the matrix element,

$$\langle \Pi_l(x) | \mathbf{J}_l | \Pi_l(x) \rangle_l = \langle \Pi_l(x) | P_l \mathbf{H}_l P_l^* | \Pi_l(x) \rangle_l = \langle P_l^* \Pi_l(x) | \mathbf{H}_l | P_l^* \Pi_l(x) \rangle_{G_l}$$

where we adopt the notation $|P_l^* \mathbf{\Pi}_l(x)\rangle = P_l^* |\mathbf{\Pi}_l(x)\rangle = |x_{n_1}\rangle + \dots + |x_{n_m}\rangle$. The assumptions on \mathbf{H}_l imply

$$\langle \mathbf{\Pi}_l(x) | \mathbf{J}_l | \mathbf{\Pi}_l(x) \rangle_l = \langle x_{n_1} | \mathbf{H}_l | x_{n_1} \rangle_{G_l} + \dots + \langle x_{n_m} | \mathbf{H}_l | x_{n_m} \rangle_{G_l} = |\mathbf{\Pi}_l^{-1}(n)| \langle x | \mathbf{H}_l | x \rangle_{G_l} = H_l(x, x)$$

where the last equality holds as $|\mathbf{\Pi}_l^{-1}(n)|$ cancels the weights in the inner product defined on G_l . Similar reasoning will give the second part of the statement. Assume y is adjacent to x such that $y \in \mathbf{\Pi}_l^{-1}(n+1) = \{y_{n_1}, \dots, y_{n_k}\}$,

$$\begin{aligned} \langle \mathbf{\Pi}_l(x) | \mathbf{J}_l | \mathbf{\Pi}_l(x) + 1 \rangle_l &= \langle P_l^* \mathbf{\Pi}_l(x) | \mathbf{H}_l | P_l^*(\mathbf{\Pi}_l(x) + 1) \rangle_{G_l} \\ &= (\langle x_{n_1} | + \dots + \langle x_{n_m} |) \mathbf{H}_l (|y_{n_1}\rangle + \dots + |y_{n_k}\rangle) \\ &= \mathbf{deg}_+(x) |\mathbf{\Pi}_l^{-1}(n)| \langle x | \mathbf{H}_l | y \rangle_{G_l} \\ &= \mathbf{deg}_+(x) H_l(x, y) \end{aligned}$$

To prove the third statement, we first observe that the previous computations verify the following equation,

$$\langle \mathbf{\Pi}_l(x) | \mathbf{J}_l | \mathbf{\Pi}_l(x) + 1 \rangle_l = \mathbf{deg}_+(x) |\mathbf{\Pi}_l^{-1}(n)| \langle x | \mathbf{H}_l | y \rangle_{G_l}$$

Similarly we can show,

$$\langle \mathbf{\Pi}_l(x) + 1 | \mathbf{J}_l | \mathbf{\Pi}_l(x) \rangle_l = \mathbf{deg}_-(y) |\mathbf{\Pi}_l^{-1}(n+1)| \langle y | \mathbf{H}_l | x \rangle_{G_l}.$$

Hence, it suffices to prove $\mathbf{deg}_-(y) |\mathbf{\Pi}_l^{-1}(n+1)| = \mathbf{deg}_+(x) |\mathbf{\Pi}_l^{-1}(n)|$. The last equality holds as both left-hand side, and the right-hand side gives the number of edges between the transversal layers $|\mathbf{\Pi}_l^{-1}(n)|$ and $|\mathbf{\Pi}_l^{-1}(n+1)|$. \square

Proof of Theorem 1. We observe

$$(\mathbf{J}_l)^k = P_l \mathbf{H}_l P_l^* \cdot P_l \mathbf{H}_l P_l^* \cdots P_l \mathbf{H}_l P_l^* = P_l (\mathbf{H}_l \mathbf{Proj}_l)^k P_l^*$$

where $P_l^* = \mathbf{Proj}_l P_l^*$ holds due to Lemma 3 and $P_l^* P_l = \mathbf{Proj}_l$ due to Lemma 5. Hence,

$$P_l e^{i T_l \mathbf{H}_l \mathbf{Proj}_l} P_l^* |0\rangle = P_l e^{i\phi} P_l^* |N\rangle \Rightarrow P_l e^{i T_l \mathbf{H}_l \mathbf{Proj}_l} |x_l\rangle = P_l e^{i\phi} |x_R\rangle$$

which implies $e^{i T_l \mathbf{H}_l \mathbf{Proj}_l} |x_R\rangle - e^{i\phi} |x_L\rangle \in \text{Ker}(P_l)$. Note that $|x_L\rangle = P_l^* |0\rangle$ and $|x_R\rangle = P_l^* |N\rangle$. By Corollary 4 and by the fact that $|x_L\rangle, |x_R\rangle \in L^2_{sym}(G_l)$ we conclude,

$$e^{i T_l \mathbf{H}_l \mathbf{Proj}_l} |x_R\rangle = e^{i\phi} |x_L\rangle$$

Let \mathbf{Proj}_l^\perp be the projection of $L^2(G_n)$ onto $(L^2_{sym}(G_l))^\perp$. We observe,

$$(\mathbf{H}_l \mathbf{Proj}_l + \mathbf{H}_l \mathbf{Proj}_l^\perp) |x_L\rangle = \mathbf{H}_l \mathbf{Proj}_l |x_L\rangle,$$

which implies $e^{i T_l \mathbf{H}_l} |x_L\rangle = e^{i\phi} |x_R\rangle$. \square

6 Conclusions and outlook.

Our construction provides an infinite set of new examples of novel geometries for which perfect quantum state transfer can be achieved. For example, using the spin-coupling values J_n in (4) for the simplest case of a spin chain, combined with our Hamiltonian construction in Proposition 1 and Theorem 1, we find perfect quantum state transfer on diamond fractals such as those shown in Figures 1 and 4. This clearly generalizes to the set of quantum systems on the graphs G_l described in Section 3. The basic projection idea is very general and applicable to many other fractal-type graphs, which allows to construct further examples. This opens up the possibility to *design* perfect quantum state transfer on fractal-like structures with special features. The existence of results for Green's functions for these structures means that other quantum information properties such as fidelity and entanglement can be studied for these fractal structures. Moreover, our approach allows to consider other transport phenomena involving linear and nonlinear, classical and quantum waves on certain graphs, quantum graphs, and fractals. This will be the subject of future research.

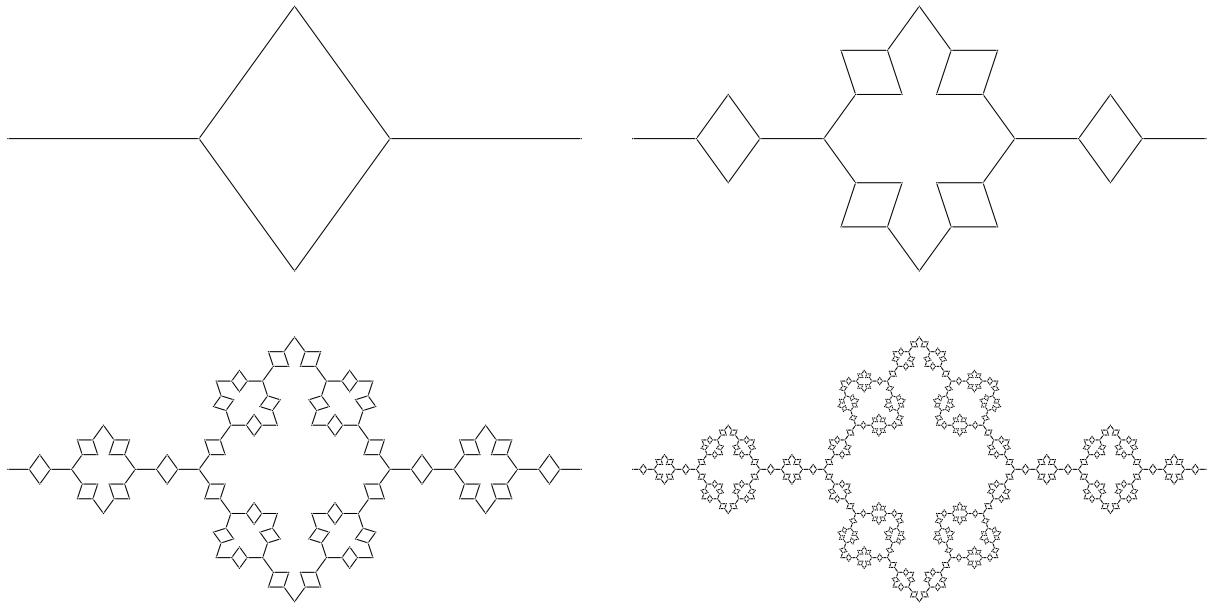


Figure 4: Diamond graphs of level 1,2,3 and 4 with uniformly bounded degree and the similarity dimension $\dim = \frac{\log 6}{\log 4}$, [19, 26, 41, 42].

7 Acknowledgments

This research was supported in part by the University of Connecticut Research Excellence Program, by DOE grant DE-SC0010339 and by NSF DMS grant 1613025. The authors are grateful to Eric Akkermans, Patricia Alonso-Ruiz and Gabor Lippner for interesting and helpful discussions.

References

- [1] Sougato Bose. Quantum communication through an unmodulated spin chain. *Physical Review Letters*, 91(20):207901, 2003.
- [2] Sougato Bose. Quantum Communication through Spin Chain Dynamics: an Introductory Overview. *Contemporary Physics*, 48:13 – 30, Feb 2007.
- [3] A Kay. A review of perfect state transfer and its applications as a constructive tool. *Int. J. Quantum Inform.*, 641(8), 2010. Preprint quant-ph/0903.4274.
- [4] Matthias Christandl, Luc Vinet, and Alexei Zhedanov. Analytic next-to-nearest-neighbor x x models with perfect state transfer and fractional revival. *Physical Review A*, 96(3):032335, 2017.
- [5] Mark Kempton, Gabor Lippner, and Shing-Tung Yau. Perfect state transfer on graphs with a potential. *Quantum Inf. Comput.*, 17(3-4):303–327, 2017.
- [6] Matthias Christandl, Nilanjana Datta, Artur Ekert, and Andrew J Landahl. Perfect state transfer in quantum spin networks. *Physical Review Letters*, 92(18):187902, 2004.
- [7] Daniel Burgarth and Sougato Bose. Conclusive and arbitrarily perfect quantum-state transfer using parallel spin-chain channels. *Physical Review A*, 71(5):052315, 2005.
- [8] Daniel Burgarth and Sougato Bose. Perfect quantum state transfer with randomly coupled quantum chains. *New journal of physics*, 7(1):135, 2005.
- [9] Peter Karbach and Joachim Stolze. Spin chains as perfect quantum state mirrors. *Physical Review A*, 72(3):030301, 2005.
- [10] Ricardo J. Angeles-Canul, Rachael M. Norton, Michael C. Opperman, Christopher C. Paribello, Matthew C. Russell, and Christino Tamon. Perfect state transfer, integral circulants, and join of graphs. *Quantum Inf. Comput.*, 10(3-4):325–342, 2010.
- [11] Rachel Bachman, Eric Fredette, Jessica Fuller, Michael Landry, Michael Opperman, Christino Tamon, and Andrew Tollefson. Perfect state transfer on quotient graphs. *Quantum Inf. Comput.*, 12(3-4):293–313, 2012.
- [12] Chris Godsil. When can perfect state transfer occur? *Electron. J. Linear Algebra*, 23:877–890, 2012.
- [13] Anna Bernasconi, Chris Godsil, and Simone Severini. Quantum networks on cubelike graphs. *Phys. Rev. A (3)*, 78(5):052320, 5, 2008.
- [14] Chris Godsil. State transfer on graphs. *Discrete Math.*, 312(1):129–147, 2012.
- [15] Luc Vinet and Alexei Zhedanov. Para-Krawtchouk polynomials on a bi-lattice and a quantum spin chain with perfect state transfer. *J. Phys. A*, 45(26):265304, 11, 2012.

- [16] Mark Kempton, Gabor Lippner, and Shing-Tung Yau. Pretty good quantum state transfer in symmetric spin networks via magnetic field. *Quantum Inf. Process.*, 16(9):Art. 210, 23, 2017.
- [17] Steve Kirkland, Darian McLaren, Rajesh Pereira, Sarah Plosker, and Xiaohong Zhang. Perfect quantum state transfer in weighted paths with potentials (loops) using orthogonal polynomials. *Linear Multilinear Algebra*, 67(5):1043–1061, 2019.
- [18] Luc Vinet and Alexei Zhedanov. How to construct spin chains with perfect state transfer. *Physical Review A*, 85(1):012323, 2012.
- [19] Leonid Malozemov and Alexander Teplyaev. Pure point spectrum of the Laplacians on fractal graphs. *J. Funct. Anal.*, 129(2):390–405, 1995.
- [20] Eric Akkermans, Gerald V Dunne, and Alexander Teplyaev. Physical consequences of complex dimensions of fractals. *EPL (Europhysics Letters)*, 88(4):40007, 2009.
- [21] B. M. Hambly and T. Kumagai. Diffusion on the scaling limit of the critical percolation cluster in the diamond hierarchical lattice. *Comm. Math. Phys.*, 295(1):29–69, 2010.
- [22] Volodymyr Nekrashevych and Alexander Teplyaev. Groups and analysis on fractals. In *Analysis on graphs and its applications*, volume 77 of *Proc. Sympos. Pure Math.*, pages 143–180. Amer. Math. Soc., Providence, RI, 2008.
- [23] Patricia Alonso Ruiz. Explicit formulas for heat kernels on diamond fractals. *Comm. Math. Phys.*, 364(3):1305–1326, 2018.
- [24] Patricia Alonso Ruiz. Heat kernel analysis on diamond fractals. *Preprint*, 2019.
- [25] Alexander Teplyaev. Harmonic coordinates on fractals with finitely ramified cell structure. *Canad. J. Math.*, 60(2):457–480, 2008.
- [26] Leonid Malozemov and Alexander Teplyaev. Self-similarity, operators and dynamics. *Math. Phys. Anal. Geom.*, 6(3):201–218, 2003.
- [27] Antoni Brzoska, Aubrey Coffey, Madeline Hansalik, Stephen Loew, and Luke G Rogers. Spectra of magnetic operators on the diamond lattice fractal. *Preprint arXiv:1704.01609*, 2017.
- [28] Martin T. Barlow and Steven N. Evans. Markov processes on vermiculated spaces. In *Random walks and geometry*, pages 337–348. Walter de Gruyter, Berlin, 2004.
- [29] Patricia Alonso-Ruiz, Michael Hinz, Alexander Teplyaev, and Rodrigo Treviño. Canonical diffusions on the pattern spaces of aperiodic delone sets. *Preprint arXiv:1801.08956*, 2018.
- [30] Benjamin Steinhurst and Alexander Teplyaev. Spectral analysis and dirichlet forms on Barlow-Evans fractals. *preprint arXiv:1204.5207*, 2018.

- [31] N. Bajorin, T. Chen, A. Dagan, C. Emmons, M. Hussein, M. Khalil, P. Mody, B. Steinhurst, and A. Teplyaev. Vibration modes of $3n$ -gaskets and other fractals. *J. Phys. A*, 41(1):015101, 21, 2008.
- [32] N. Bajorin, T. Chen, A. Dagan, C. Emmons, M. Hussein, M. Khalil, P. Mody, B. Steinhurst, and A. Teplyaev. Vibration spectra of finitely ramified, symmetric fractals. *Fractals*, 16(3):243–258, 2008.
- [33] Eric Akkermans, Gerald V Dunne, and Alexander Teplyaev. Thermodynamics of photons on fractals. *Physical review letters*, 105(23):230407, 2010.
- [34] Eric Akkermans, Olivier Benichou, Gerald V Dunne, Alexander Teplyaev, and Raphael Voituriez. Spatial log-periodic oscillations of first-passage observables in fractals. *Physical Review E*, 86(6):061125, 2012.
- [35] Eric Akkermans, Joe P Chen, Gerald Dunne, Luke G Rogers, and Alexander Teplyaev. Fractal AC circuits and propagating waves on fractals. *to appear in the 6th Cornell Fractals Conference Proceedings, arXiv:1507.05682*, 2019.
- [36] Eric Akkermans. Statistical mechanics and quantum fields on fractals. In *Fractal geometry and dynamical systems in pure and applied mathematics. II. Fractals in applied mathematics*, volume 601 of *Contemp. Math.*, pages 1–21. Amer. Math. Soc., Providence, RI, 2013.
- [37] Gerald V. Dunne. Heat kernels and zeta functions on fractals. *J. Phys. A*, 45(37):374016, 22, 2012.
- [38] Patricia Alonso-Ruiz, Daniel J. Kelleher, and Alexander Teplyaev. Energy and Laplacian on Hanoi-type fractal quantum graphs. *J. Phys. A*, 49(16):165206, 36, 2016.
- [39] Michael Hinz and Melissa Meinert. On the viscous Burgers equation on metric graphs and fractals. *Journal of Fractal Geometry, to appear. arXiv:1712.05472*, 2019.
- [40] Gábor Szegő. *Orthogonal polynomials*. American Mathematical Society, Providence, R.I., fourth edition, 1975. American Mathematical Society, Colloquium Publications, Vol. XXIII.
- [41] Bernhard Krön and Elmar Teufl. Asymptotics of the transition probabilities of the simple random walk on self-similar graphs. *Trans. Amer. Math. Soc.*, 356(1):393–414, 2004.
- [42] Urs Lang and Conrad Plaut. Bilipschitz embeddings of metric spaces into space forms. *Geom. Dedicata*, 87(1-3):285–307, 2001.